International Immunopharmacology 181 (2026) 116744

Contents lists available at ScienceDirect

International Immunopharmacology

journal homepage: www.elsevier.com/locate/intimp

PTK6 promotes ferroptosis resistance and CD8$^+$ T cell exhaustion in pancreatic tumors via reprogramming glucose and lipid metabolism

Rui Zheng [a,*,1], Si Wang [b], Dan Li [a], Xing Tian [c], Lifeng Sun [c], Jiao Wang [a], Yuchang Wang [d], Xuyi Pan [d], Yifan Liang [d], Zhihang Yang [a,*]

[a] Department of Physiology, School of Basic Medicine, Shenyang Medical College, Shenyang 110034, China
[b] Department of Pathogenic Microbiology, School of Basic Medical Science, China Medical University, Shenyang 110122, China
[c] Liaoning Province Key Laboratory for Phenomics of Human Ethnic Specificity and Critical Illness, Shenyang Medical College, Shenyang 110034, China
[d] Shenyang Key Laboratory for Phenomics, Shenyang Medical College, Shenyang 110034, China

ARTICLE INFO

Editor: Dr. Amorette Barber

Keywords:
Pancreatic tumor
Tumor microenvironment
PTK6
Glucose and lipid metabolism
CD8$^+$ T cell exhaustion

ABSTRACT

Pancreatic ductal adenocarcinoma (PDAC) is a malignant tumor associated with poor prognosis and high mortality. The distinct metabolic reprogramming of nutrients in PDAC fosters an immunosuppressive tumor immune microenvironment (TIME) and compromises the efficacy of immunotherapy. Protein tyrosine kinase 6 (PTK6) is highly expressed in multiple solid tumors and contains a short N-terminal region featuring an SH2 domain capable of lipid binding, suggesting its involvement in lipid metabolic reprogramming within the malignant tumor microenvironment. Using PTK6-knockout mouse models and lipidomic sequencing, we investigated how PTK6 drives metabolic dysregulation and immune effector exhaustion in pancreatic tumors. Our findings uncover a "dual driver" role for PTK6 in PDAC progression: While it enhances cancer cell resistance to ferroptosis by the reprogramming lipid metabolism, it also promotes CD8$^+$ T cell exhaustion through upregulating PD-1 and Tim-3 expression, ultimately driving immunosuppression. In summary, these findings identify PTK6 as a potential biomarker in PDAC and reveal a previously unrecognized role of PTK6 in linking tumor lipid metabolism to CD8$^+$ T cell exhaustion. These data suggest that PTK6 may represent a candidate mechanistic target for further therapeutic exploration.

1. Introduction

Pancreatic cancer (PC) is a highly lethal malignancy whose incidence has doubled over the past two decades. With an overall 5-year survival rate of only 9%, it remains one of the digestive system tumors with the poorest prognosis [1,2]. Pancreatic ductal adenocarcinoma (PDAC) is the most common subtype, accounting for more than 90% of all pancreatic cancer cases [3]. Currently, surgical resection remains the only curative treatment option for pancreatic cancer. However, most patients are diagnosed at an advanced stage, with only 15–20% eligible for surgery. Even among those who undergo successful resection, local recurrence and metastasis remain frequent [4,5]. *KRAS* and *TP53* mutations are commonly identified in the majority of pancreatic cancer patients. Oncogenic KRAS activates downstream effectors and promotes neoplastic transformation of pancreatic acinar cells. Concurrently, *TP53* mutation compromises genomic integrity, thereby driving pancreatic cancer progression toward high-grade disease [6]. The complexity of the pancreatic tumor microenvironment (TME) contributes to tumor spatial heterogeneity. The composition of stromal cells often dictates the evolutionary stage of the tumor and the cellular context of PDAC progression, whereas KRAS-transformed epithelial cells drive rapid remodeling of the tumor stroma. These observations point to a close interplay between oncogenic signaling in pancreatic epithelial cells and the stromal microenvironment [7,8].

A critical determinant of the high mortality rate of pancreatic cancer is its acquired immune privilege, driven by an immunosuppressive tumor microenvironment, poor T-cell infiltration, and a low mutational burden [9]. In many clinical evaluations of immunotherapy strategies—including immune checkpoint inhibitors, cancer vaccines, and combination regimens—no significant clinical benefit has been observed [10]. Therefore, identifying more effective prognostic biomarkers remains a major focus of research, which holds significant

* Corresponding authors.
E-mail addresses: zhengruill@163.com (R. Zheng), yzhsmc@symc.edu.cn (Z. Yang).
[1] Lead contact.

https://doi.org/10.1016/j.intimp.2026.116744
Received 10 March 2026; Received in revised form 15 April 2026; Accepted 23 April 2026
Available online 28 April 2026

implications for early diagnosis of pancreatic cancer, informing clinical treatment strategies, and improving patient survival.

Protein tyrosine kinase 6 (PTK6), also known as breast tumor kinase or Src-related intestinal kinase, is a non-receptor tyrosine kinase [11]. The *PTK6* gene is located on human chromosome 20q13.3 and encodes a 451 amino acid protein. PTK6 shares structural features with SRC family kinases, including a unique short N-terminal region, followed by an SH2 domain involved in lipid binding and an SH3 domain responsible for substrate recognition [12–14]. PTK6 expression is low or undetectable in normal breast and ovarian tissues but is frequently overexpressed in a variety of malignant tumors [15–18]. PTK6 has been shown to promote pancreatic cancer cell migration and invasion via ERK1/2 signaling. Suppression of endogenous PTK6 overexpression enhances gemcitabine-induced DNA damage and promotes apoptosis in pancreatic tumors in mouse models [19,20]. Nevertheless, the role of PTK6 in pancreatic cancer remains incompletely characterized. Elucidating how PTK6 modulates the pancreatic tumor immune microenvironment is therefore of critical importance, as this may open new avenues for improving patient prognosis and guiding clinical immunotherapy strategies.

2. Materials and methods

2.1. Cell culture and siRNA

The C57BL/6 mouse pancreatic cancer cell line Panc02 was purchased from the Cell Bank of the Chinese Academy of Sciences (Shanghai, China) and cultured in DMEM supplemented with 10% fetal bovine serum and 1% penicillin/streptomycin at 37 °C and 5% CO_2 in a humidified incubator.

The small interfering RNA (siRNA) targeting mouse PTK6 and negative control siRNA were synthesized by Hesheng Gene Technology Co., Ltd. (Beijing, China). The sense strand sequence of PTK6 siRNA was 5'-GCGUGACUCUGAUGAGAAAGC-3′. 1×10^5 Panc02 cells per well were seeded in 6-well plates (using DMEM medium without antibiotics and serum). Cells were transfected with siRNA using Lipofectamine™ 3000 according to the manufacturer's instructions. siRNA-lipid complexes were prepared and added to the culture medium with gentle mixing. After 48 h, cells were collected for Western blot analysis. Panc02 cells were subjected to siRNA-mediated PTK6 gene knockdown as described above.

2.2. Experimental animal models

All animal experiments were approved and performed in accordance with the guidelines of the Institutional Animal Care and Use Committee of China Medical University. C57BL/6 (WT) mice were purchased from Beijing Huafukang Biotechnology Co. PTK6-targeted knockout mice ($PTK6^{-/-}$) in C57BL/6 gene background were generated utilizing the CRISPR/Cas9 method by Cyagen Biosciences Co., Ltd. (Guangzhou, China). Mice had fresh water and autoclaved food and were kept at the Laboratory Animal Center, China Medical University throughout all the experiments.

To establish orthotopic and subcutaneous murine models of pancreatic ductal adenocarcinoma (PDAC), 2×10^5 siPTK6-transfected Panc02 cells were resuspended with Matrigel at a 1:1 ratio. For the orthotopic model, cells were injected into the tail of the pancreas; for the subcutaneous model, cells were inoculated into the right axilla of mice. Tumor volumes were calculated using the formula: 0.5 × lengths × width × width.

2.3. Bioinformatics analysis

The transcriptomic and clinical data for pancreatic cancer samples were obtained from The Cancer Genome Atlas (TCGA) database (https://xena.ucsc.edu) and The Gene Expression Omnibus (GEO) database (https://www.ncbi.nlm.nih.gov/geo). Normal tissue transcriptomic profiles were sourced from The Genotype-Tissue Expression (GTEx) Project through the UCSC Xena browser (https://xena.ucsc.edu) to establish a baseline for gene expression. RNA-seq expression data for TCGA and GTEx were obtained from the UCSC Xena platform, processed using the TOIL RNA-seq Recompute pipeline. This pipeline uniformly reprocessed raw RNA-seq data from TCGA and GTEx using the same computational workflow, and applied ComBat batch effect correction to remove technical variations between datasets while preserving biological differences. The batch-corrected normalized expression data were used for subsequent analyses [21].

For the single-cell clustering analysis, the pancreatic cancer dataset PAAD_GSE111672 was retrieved from The Tumor Immune Single-cell Hub 2 (TISCH2, http://tisch.comp-genomics.org/). This dataset encompasses pre-processed gene expression matrices and curated cell-type annotations, facilitating downstream clustering and tumor microenvironment characterization. Gene expression profiles from the TCGA and GTEx datasets were merged and subsequently normalized, yielding a combined cohort of 171 normal samples and 179 tumor samples. Differentially expressed genes (DEGs) were identified using a threshold of absolute log2 fold change ($|Log2FC| > 2.0$ and an adjusted *P*-value (adj. *P*) < 0.01. Based on the median expression value of PTK6, patients were stratified into high- and low-expression groups. The CIBERSORT algorithm, a deconvolution approach, was used to estimate the relative abundances of 22 human immune cell subsets in each patient sample. Associations between PTK6 expression and clinicopathological features—including sex, age, tumor grade, disease stage, and TNM classification—were then evaluated using patient clinical data. Gene Set Enrichment Analysis (GSEA, version 4.1.0) was performed to identify significantly enriched biological functions and signaling pathways.

A prognostic gene signature was constructed using LASSO Cox regression analysis to identify the most informative prognostic genes from the candidate gene set. The analysis was performed using the glmnet package in R. Ten-fold cross-validation was conducted to select the optimal λ value that yielded the minimum cross-validation error. The risk score for each patient was calculated as a linear combination of gene expression values weighted by the LASSO-derived coefficients, using the formula:

Risk score = Σ(expression_i × coefficient_i).

Genes with nonzero regression coefficients were included in the final prognostic model. The prognostic model was developed in the training cohort (TCGA) and validated in an independent external cohort (GSE28735) to verify its stability and clinical utility. Survival differences between risk groups were compared using Kaplan–Meier curves with log-rank tests. The predictive accuracy was evaluated using time-dependent ROC analysis.

2.4. Lipidomics metabolome analysis using LC–MS/MS

Wild-type or $PTK6^{-/-}$ C57BL/6 mice orthotopic pancreatic tumor tissues preserved in RNA protection solution (RNA-EZ Reagents RNA-Be-Locker A) was frozen in liquid nitrogen before lipidomice metabolome analysis by Shanghai Zhongke New Life Biotechnology Co., Ltd.

2.5. Real-time PCR

Total RNA was extracted using TRIzol reagent. Reverse transcription and PCR were performed according to the manufacturer's protocols for the PrimeScriptTM RT Master Mix and the TB Green® Premix Ex Taq™ (Tli RNaseH Plus). Results are normalized to β-actin and presented as fold mRNA expression ($2^{-\triangle\triangle CT}$). The primer sequences are detailed in the supplementary Materials and Methods.

2.6. Western blot

Western blotting was performed as previously described [22]. Rabbit anti-PTK6 antibody (K005293P, 1:500, Solarbio), Rabbit anti-4-HNE

antibody (68538–1-Ig, 1:500, Proteintech), and Rabbit anti-GPX4 antibody (67763–1-Ig, 1:500, Proteintech) were used in this study. The immunocomplexes were visualized with the BeyoECL Plus Chemiluminescent Substrate. Protein band intensity was quantified with Image J software.

2.7. Immunohistochemistry assay

Tumor sections were incubated with the primary antibody against PTK6, CD27, CD86, CXCR1 and CCR5, followed by incubation with biotinylated secondary antibodies (Santa Cruz Biotechnology). Diaminobenzidine substrate was used to reveal immunoreactive products. The signal strength in tumor tissues was calculated using Image J software.

2.8. Preparation of single-cell suspension from tumor mass

Pancreatic tumor tissues were mechanically dissociated and then digested with 0.25% trypsin for 10 min at 37 °C on a rocking platform. The spleen was gently ground to prepare a homogeneous single-cell suspension. After red blood cell lysis, cells from both tissues were resuspended in RPMI 1640 medium and counted.

2.9. Flow cytometry

Isolated cells were incubated with anti-mouse CD16/32 monoclonal antibody to block Fc receptors. Then, the cells were then stained with fluorescence-conjugated antibodies against surface antigens for 30 min at 4 °C. For intracellular cytokine staining, cells were stimulated with PMA (25 ng/mL, Sigma, P1585), ionomycin (1 μg/mL, Sigma, I0634), and brefeldin A (10 μg/mL, Sigma, B5936) for 4 h at 37 °C prior to staining.

2.10. Transmission Electron microscope (TEM)

TEM analysis was conducted on both orthotopic pancreatic tumor tissues harvested from mice or in vitro cultured cells, performed by Shiyanjia Lab (www.shiyanjia.com).

2.11. Statistics

SPSS 22.0, GraphPad Prism 7 and R language statistical software were used for data analysis. All values were displayed as mean ± SEM. Due to the small sample size ($n = 5$ per group), normality was assessed by Shapiro-Wilk test and Q-Q plots, with no evidence of severe deviation. Homogeneity of variances was confirmed by Levene's test ($p > 0.05$). Student's *t*-test was applied to analyze the difference between the two groups. Group comparisons were performed using one-way ANOVA followed by Tukey's post hoc test. For lipidomic data, multiple hypothesis testing was corrected using the Benjamini–Hochberg false discovery rate (FDR) method, with adjusted $p < 0.05$ considered statistically significant. Orthogonal partial least-squares discriminant analysis (OPLS-DA) was performed using R package ropls. Model validity was assessed by permutation testing ($n = 200$ permutations) to evaluate overfitting. The model was considered valid when the R^2 and Q^2 values from permuted data were lower than those from the original model. Statistical significance: $^*p < 0.05$, $^{**}p < 0.01$, $^{***}p < 0.001$ and $^{****}p < 0.0001$; n.s., not significant.

3. Results

3.1. Increased PTK6 expression is positively associated with poor prognosis in patients

Analysis of the TCGA-PAAD and GTEx datasets revealed significantly higher PTK6 expression in pancreatic tumor tissues than in normal pancreatic tissues (Fig. 1A-B). Kaplan-Meier survival analysis showed that elevated PTK6 expression was negatively correlated with both overall survival (OS) and disease-free survival (DFS), suggesting its potential as an independent prognostic factor (Fig. 1C-D). Moreover, correlation analysis between PTK6 expression and clinicopathological characteristics revealed significant associations with patient sex, pathological subtype, and tumor grade. (Fig. 1E).

To further validate the bioinformatics findings, 2×10^5/mL Panc02 pancreatic cancer cells were orthotopically implanted into the pancreatic tail of C57BL/6 mice. Pancreatic tumor tissues were harvested 14 days post-implantation. We found that both PTK6 mRNA and protein expression levels were significantly higher in pancreatic tumor tissues from wild-type tumor-bearing mice compared to normal pancreatic tissues from control mice (Fig. 1F-G, Fig. 2A). PTK6 was transiently knocked down in Panc02 cells by siRNA transfection. (Fig. S1A). Subsequently, 2×10^5/mL siPTK6-Panc02 cells were orthotopically implanted into the pancreatic tail of $PTK6^{-/-}$ C57BL/6 mice to monitor survival. Separately, the same cell dose was injected into the right axilla of $PTK6^{-/-}$ C57BL/6 mice, where tumor weight and volume were evaluated relative to wild-type C57BL/6 controls receiving Panc02 cells. We observed that PTK6 reduced the survival rate of tumor-bearing mice and was associated with increased tumor weight and volume (Fig. 2B-C). These results suggest that PTK6 promotes pancreatic tumor growth and serves as a negative prognostic indicator for patient survival.

3.2. PTK6 limits effector T cell infiltration in the tumor microenvironment and reshapes the systemic immune landscape

To investigate the role of PTK6 in the tumor immune microenvironment of PDAC, the CIBERSORT algorithm was used to deconvolute the immune cell composition of each PDAC sample. Samples were then stratified into high- and low-PTK6 expression groups using the median expression level as the cutoff. The correlation between PTK6 expression and the infiltration levels of 22 human immune cell subsets was subsequently analyzed. PTK6 expression levels were associated with distinct patterns of immune cell infiltration. Analysis of TCGA pancreatic cancer transcriptomic data showed that high PTK6 expression was associated with lower infiltration levels of naïve B cells, plasma cells, $CD8^+$ T cells, activated memory $CD4^+$ T cells, and monocytes, but higher infiltration levels of memory B cells, resting memory $CD4^+$ T cells, and M0 macrophages (Fig. 2D, Supplementary Table 1). Differential expression of PTK6 showed a negative correlation with multiple key immune effector regulatory factors (Fig. S1B). Chemokines are well-established regulators of cell trafficking into and out of the tumor microenvironment across various physiological and pathological settings. In this study, chemokine levels were also found to be negatively correlated with high PTK6 expression (Fig. S1C) [23]. These results collectively confirm that PTK6 overexpression serves as an indicator of a suppressed tumor immune microenvironment.

Based on the bioinformatics analysis, we focused on effector T cell infiltration within the pancreatic tumor microenvironment. Single-cell suspensions were prepared from orthotopic pancreatic tumor tissues and spleens of tumor-bearing mice and then analyzed by flow cytometry. (Fig. S1D). As shown in Fig. 3, PTK6 expression was associated with a marked reduction in the number of tumor-infiltrating $CD8^+$ and $CD4^+$ T cells within pancreatic tumor tissues, as well as attenuated systemic immune responses (Fig. 3A-B). In addition, the expression levels of major immune effector molecules and chemokines in effector T cell populations were decreased (Fig. S2A). Collectively, these findings suggest that PTK6 suppresses the anti-tumor function of effector T cells.

3.3. PTK6 impairs tumor-infiltrating $CD8^+$ T cell function and reduces immunotherapy response

Since PTK6 primarily modulates the percentage of T cells in pancreatic ductal adenocarcinoma, antigen-specific $CD8^+$ T cell-

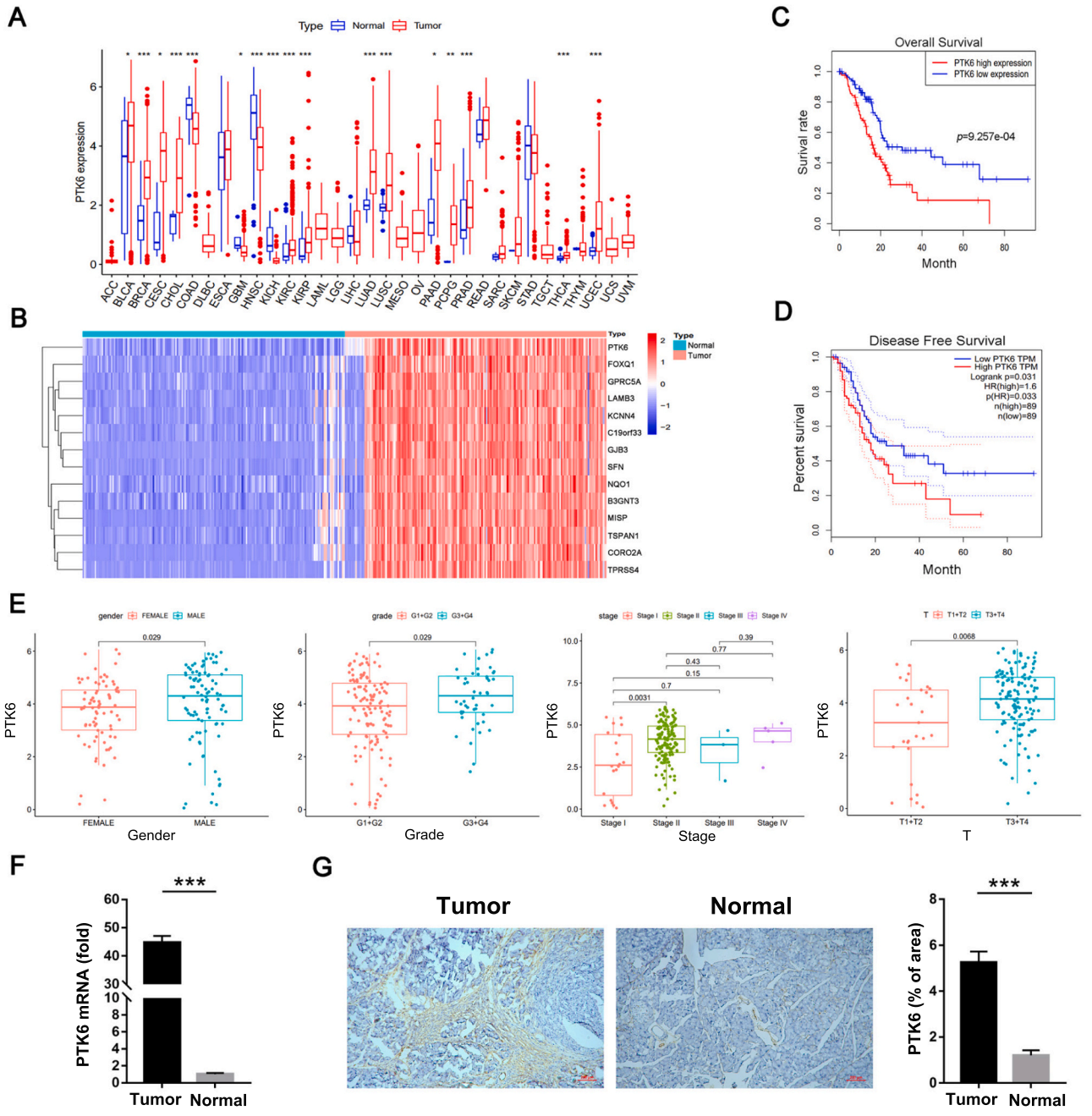

Fig. 1. Protein tyrosine kinase 6 (PTK6) is up-regulated in tumor tissues and correlates with the poor prognosis of patients with PDAC. (A) Expression changes of PTK6 in cancer genome database of 33 tumor types. (B) The differential expression of PTK6 in normal ($n = 171$) and pancreatic cancer tissue ($n = 179$) in the TCGA and GTEx databases. (C and D) Comparison of OS (C) and DFS (D) in patients with PDAC expressing high (>median level) or low (<median level) PTK6 expression in the TCGA database. (E) Correlation analysis between PTK6 and clinical pathological patterns in TCGA database. (F) Real-time PCR analysis of *PTK6* expression in tumor tissues. (G) Immunohistochemical staining and quantification of PTK6 protein levels in pancreatic tumor tissues. TCGA, The Cancer Genome Atlas; PAAD, Pancreatic adenocarcinoma. $^*p < 0.05$, $^{**}p < 0.01$, $^{***}p < 0.001$ by Student *t*-test and were presented as mean ± SEM. $n = 5$ mice per group. Scale bars = 200 μm.

mediated cytotoxicity plays a critical role in tumor eradication and the extension of patient survival [24]. This prompted us to further investigate the mechanism by which PTK6 affects the biological function of $CD8^+$ T cells. Immune-related gene expression data were extracted from the TCGA and GEO (GSE28735) databases. Differential gene expression analysis of $CD8^+$ T cells within the pancreatic tumor microenvironment was performed using single-cell clustering (PAAD_GSE111672).

The intersection of these differentially expressed genes with the aforementioned immune-related genes was identified, followed by univariate Cox analysis, which screened out 33 high-risk prognostic genes for pancreatic cancer (Fig. S2B—D, Supplementary Table 2). LASSO Cox regression analysis was performed, and a 10-fold cross-validation was applied to mitigate overfitting. With an optimal lambda value of 0.0368, ten key variables were identified (SPP1, AGT, HBEGF, DEFB1, S100A14, KLRC2, TNFSF10, NAMPT, PLAU, and GRAP2) (Fig. 4A). Patients were stratified into high- and low-risk groups based on the median risk score derived from the model. Pancreatic cancer patients showed distinct prognostic classification in both the

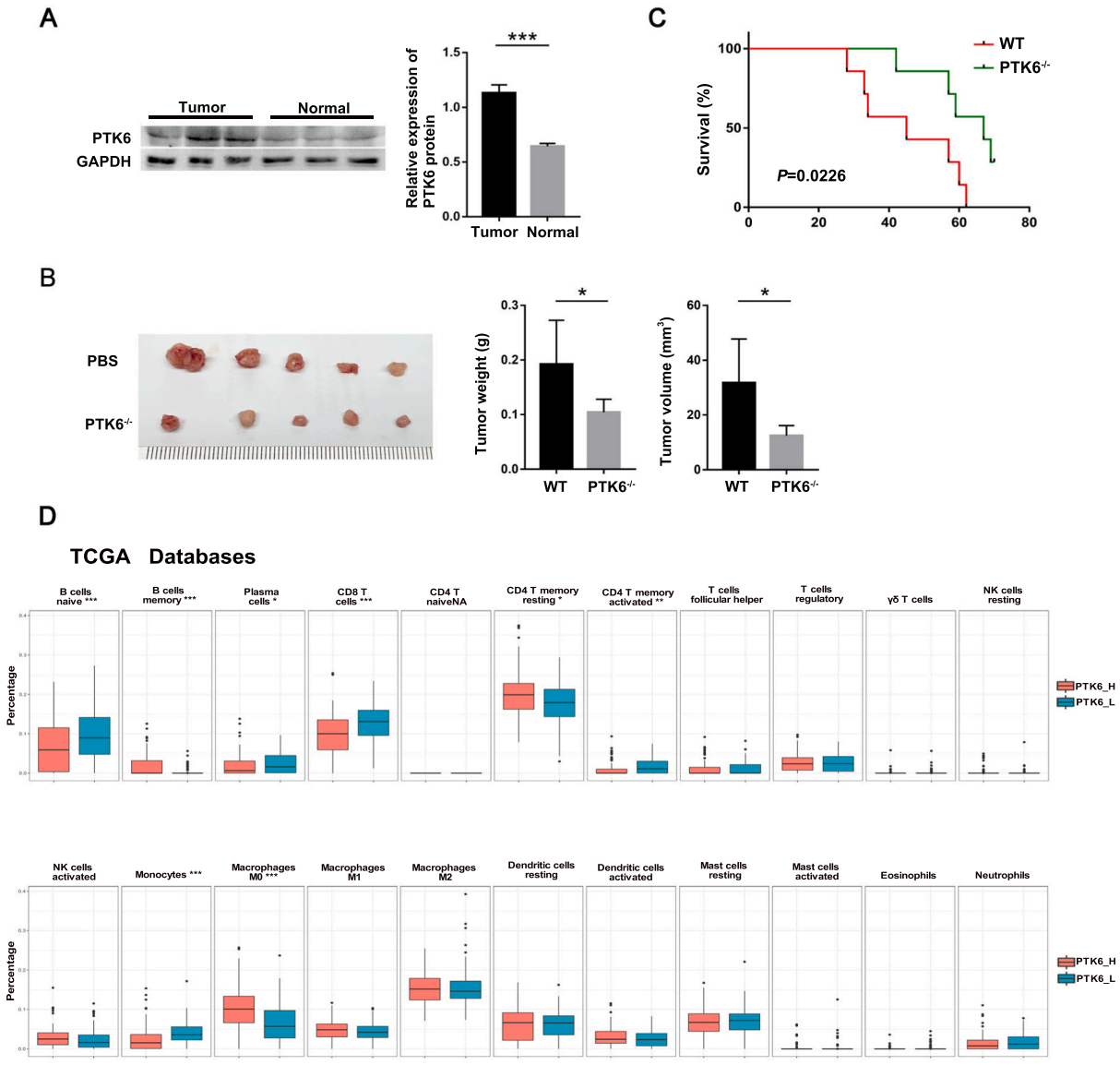

Fig. 2. PTK6 contributes to the progression of PDAC. (A) Western blot analysis and quantification of PTK6 protein levels in tumor tissues. (B) Tumor weight and volume in PTK6$^{-/-}$ C57BL/6 mice bearing siPTK6-Panc02 xenografts in the right axilla. Wild-type C57BL/6 mice implanted with Panc02 cells were used as controls. Tumors were harvested and measured at the endpoint. (C) Kaplan-Meier survival curve showing the survival of tumor-bearing mice after orthotopically implantation of tumor cells in the pancreatic tail. (D) CIBERSORT is a deconvolution algorithm used to evaluates the proportion of 22 tumor-infiltrating lymphocyte subpopulations influenced by PTK6 expression. *$p < 0.05$, ***$p < 0.001$ by Student *t*-test and were presented as mean ± SEM. n = 5–8 mice per group.

training cohort (TCGA database) and the validation cohort (GSE28735). In the training cohort, the high-risk group ($n = 86$) and the low-risk group (n = 86) exhibited overall survival (OS) of (13.51 ± 1.011) months and (24.16 ± 2.034) months, respectively ($p < 0.01$) (Fig. 4B). In the validation cohort, the high-risk group ($n = 20$) and the low-risk group ($n = 22$) showed OS of (4.517 ± 0.653) months and (9.002 ± 1.098) months, respectively ($p < 0.01$) (Fig. 4C). Patients with low expression of the model genes *TNFSF10* and *PLAU* exhibited a favorable prognosis, whereas high expression of *GRAP2* was associated with poor clinical outcomes (Fig. S3A-B). Univariate Cox regression analysis identified age, tumor grade, and risk score as significant prognostic factors associated with poor outcomes. In multivariate analysis, age and risk score remained independent risk factors for prognosis (Fig. 4D, Supplementary Table 3). To evaluate the sensitivity and specificity of the prognostic risk score, time-dependent ROC analysis was performed, yielding an area under the curve (AUC) of 0.79 for predicting 5-year survival. This result indicates that the genes comprising the model serve as highly reliable prognostic biomarkers for PDAC (Fig. 4E).

Gene Set Enrichment Analysis (GSEA) revealed that several biological pathways, including Cell cycle, DNA replication, P53 signaling pathway, Pyrimidine metabolism, Pentose phosphate pathway, and Steroid hormone biosynthesis, were significantly enriched in the high-risk prognostic group (Fig. 4F, Supplementary Table 4). PTK6 expression was elevated in the high-risk group and showed a positive correlation with the patient risk score (Fig. 4G). Within the tumor immune microenvironment of the high-risk patient group, infiltration levels of B cells, plasma cells, CD8$^+$ T cells, activated memory CD4$^+$ T cells, and resting NK cells were decreased, whereas M0 and M1 Macrophages were significantly elevated (Fig. S4A). Further analysis of immune subtype infiltration within CD8$^+$ T cells revealed that the Wound Healing (C1),

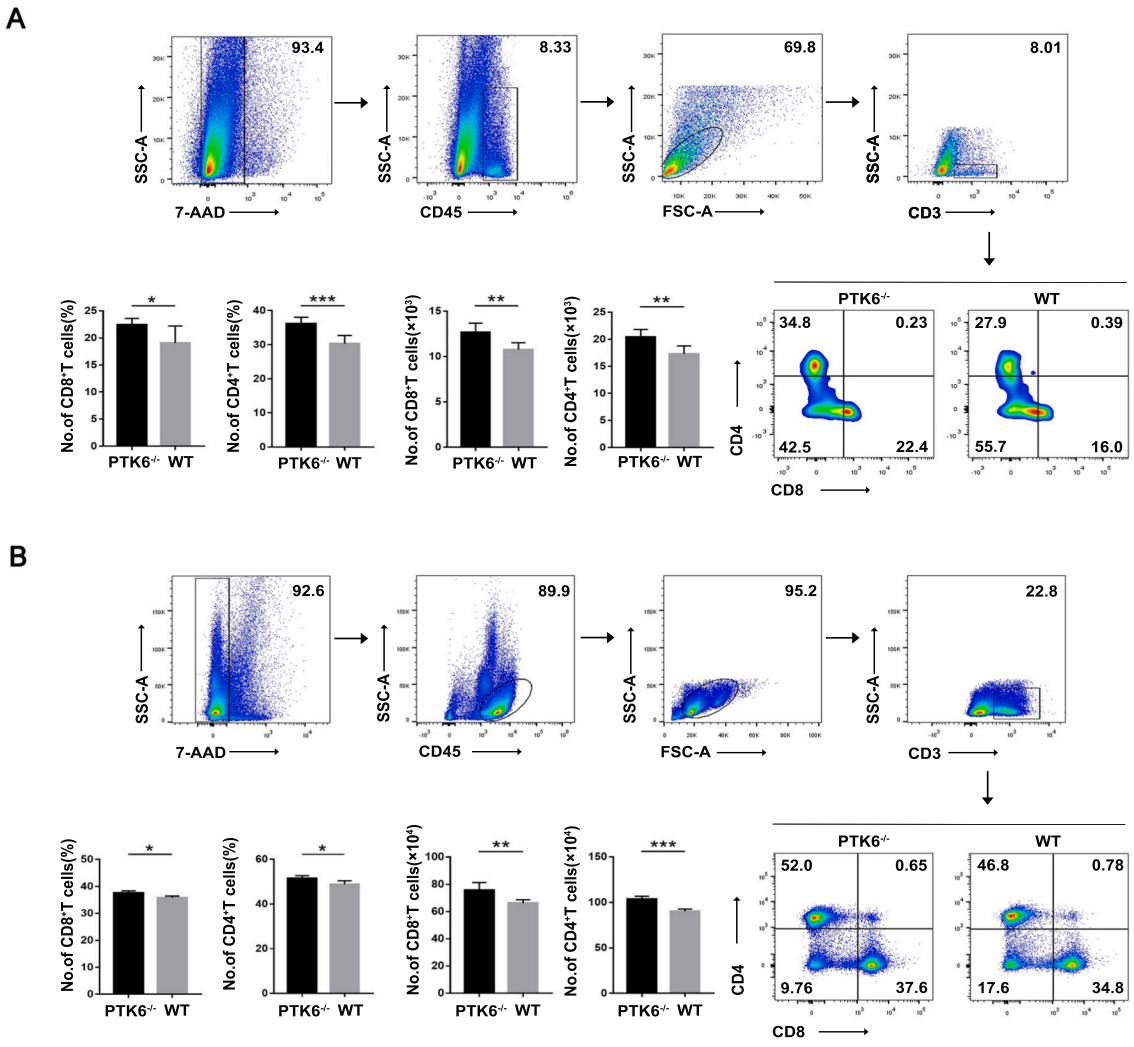

Fig. 3. PTK6 affects T cell infiltration in tumor tissue. (A and B) The percentage and absolute numbers of $CD4^+$ T cells and $CD8^+$ T cells in pancreatic tumor tissues (A) and spleens (B). $^*p < 0.05$; $^{**}p < 0.01$; $^{***}p < 0.001$ by Student *t*-test and were presented as mean ± SEM. n = 5–8 mice per group.

IFN-γ-dominant (C2), and TGF-β-dominant (C6) subtypes were predominantly enriched in the high-risk group, whereas the Inflammatory (C3) subtype was more prevalent in the low-risk group (Fig. S4B).

3.4. Metabolomic profiling revealed that PTK6 modulates characteristic metabolic alterations during pancreatic tumor progression

Given the role of PTK6 in driving immunosuppression and promoting tumorigenesis, we further investigated its potential mechanisms in regulating pancreatic tumor metabolism. First, based on the median expression level of PTK6 in TCGA tumor samples, Gene Set Enrichment Analysis (GSEA, version 4.1.0) was employed to identify the most significantly altered key pathways and core related genes between patient groups classified by PTK6 expression [25]. The results showed that the high PTK6 expression group was predominantly enriched in carbohydrate and lipid metabolism-related processes, including fructose_and_mannose_metabolism, glycosphingolipid_biosynthesis_lacto_and_neolacto_series, pentose_phosphate_pathway, glycerophospholipid_metabolism, and linoleic_acid_metabolism (Fig. S4C, Supplementary Table 5). PTK6 expression was positively correlated with the expression of genes involved in glycolysis and lipid metabolism (Fig. S5A).

Pancreatic tumor tissues were collected from mice bearing orthotopic pancreatic tumors for lipidomic analysis and lipid metabolite detection. A total of 45 lipid subclasses and 3820 lipid molecules were identified (Fig. S5B). Principal Component Analysis (PCA) of the lipidomic data revealed a clear separation between groups, with PCA1 and PCA2 accounting for 38.6% and 21.3% of the total variance, respectively, indicating substantial alterations in lipid profiles (Fig. 5A). An Orthogonal Partial Least Squares-Discriminant Analysis (OPLS-DA) model was applied to assess the separation between groups. The model

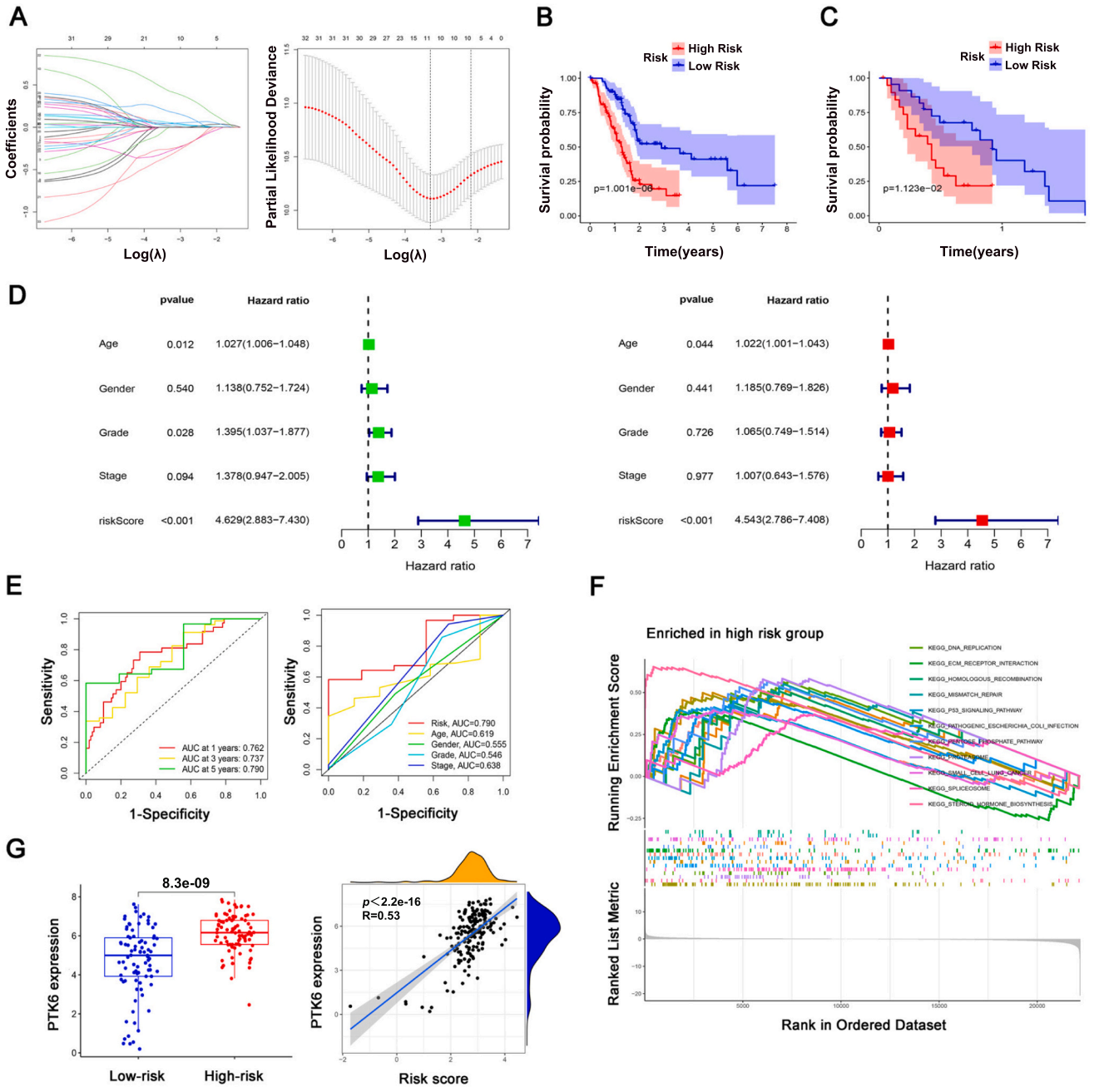

Fig. 4. PTK6 downregulation tumor-infiltrating CD8$^+$ T cell function. (A) Variables selected by the LASSO analysis and the distribution of their coefficients ($n = 10$). (B and C) Kaplan-Meier survival curve analysis of OS in the training cohort (B) and validation cohort (C). (D) Risk score and clinical characteristics of univariate (green) and multivariate (red) Cox regression analyses. (E) Time-dependent ROC curves of risk assessment and clinical parameters predicting 5-year survival in patients with pancreatic cancer. AUC, area under the curve. (F) GSEA enrichment analysis of high-risk groups. NSE, normalized enrichment score. (G) Differences in PTK6 expression and risk correlation between high-risk group (red) and low-risk group (blue). (For interpretation of the references to colour in this figure legend, the reader is referred to the web version of this article.)

parameters (R2Y = 0.994, Q2 = 0.636) indicated a stable and reliable model without overfitting (Fig. 5B). The OPLS-DA score plot demonstrated distinct lipidomic signatures between groups (Fig. 5A). Differential lipids were screened using multivariate statistical analysis based on the criteria of OPLS-DA VIP > 1 and P value <0.05. A heatmap displays the 61 lipid molecules that met these criteria (Fig. 5C).

To further validate the lipidomic findings, we examined key metabolic enzymes and metabolites in pancreatic tumor tissues of PTK6$^{-/-}$ mice. Compared with wild-type mice, PTK6$^{-/-}$ mice showed significantly reduced activities of lactate dehydrogenase, pyruvate dehydrogenase, and hexokinase, accompanied by a marked decrease in lactate levels. Concurrently, the activity of fatty acid synthase (FASN), as well as the levels of free fatty acids and triglycerides, were also lower in PTK6$^{-/-}$ tumor tissues (Fig. S5C). Furthermore, levels of reduced glutathione (GSH), the GSH/GSSG ratio, the NADPH/NADP$^+$ ratio, and Na$^+$-K$^+$ ATPase activity were all decreased (Fig. S5D). These results lead us to hypothesize that PTK6 may promote tumor energy supply by remodeling tumor glucose and lipid metabolism. Additionally, by

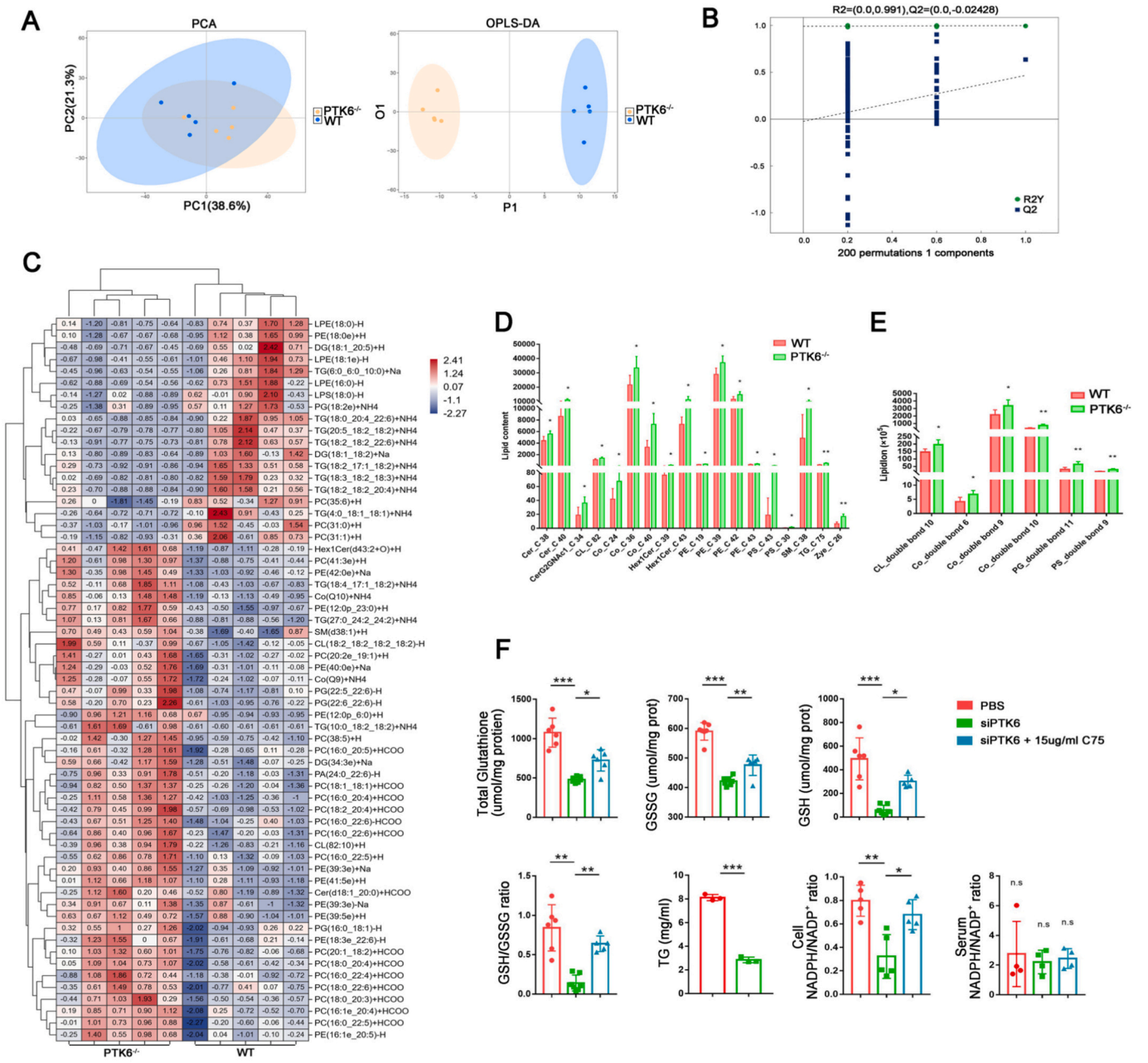

Fig. 5. Metabolic Characterization and Multivariate Data Analysis of the Lipidome in Mouse Pancreatic Tumor Tissues. (A) Principal Component Analysis (PCA) and Orthogonal Partial Least Squares Discriminant Analysis (OPLS-DA) between the two groups. (B) Permutation tests for OPLS-DA score plots. (C) The heatmap depicts differentially abundant lipid molecules between the two groups. (D) The total double bond count in the two fatty acyl chains was used to distinguish the difference in lipid saturation between the two groups. (E) Total carbon number of the fatty acyl chains was used to determine lipid subclass chain length between the two groups. (F) Key parameters of redox homeostasis (Total glutathione, GSH, GSSG, GSH/GSSG ratio, NADPH/NADP$^+$ ratio) and energy metabolism (Na^+-K^+ ATPase activity, Ca^{2+}-Mg^{2+} ATPase activity) in pancreatic tumor cells were measured using commercial kits. *$p < 0.05$; **$p < 0.01$; ***$p < 0.001$. Student's *t*-test was used for comparison of two groups, one-way ANOVA, was used for comparison of three groups (mean ± SEM).

reducing lipid accumulation, PTK6 could alter the susceptibility of pancreatic tumors to ferroptosis, while influencing immune responses through the upregulation of sterol molecules such as cholesterol, zymosterol ester (ZyE), and stigmasteryl ester (StE).

To elucidate the downstream signaling pathway through which PTK6 regulates lipid and glucose metabolism, we examined AKT and STAT3 phosphorylation in Panc02 cells with PTK6 knockdown alone or in combination with AKT agonis (SC79) or STAT3 agonis (Colivelin). As shown in Fig. S6A, PTK6 knockdown led to a significant reduction in the p-AKT/AKT ratio, while the p-STAT3/STAT3 ratio remained unchanged in PTK6-knockdown cells and was only substantially decreased following Colivelin treatment. These findings demonstrate that PTK6 selectively activates the AKT signaling pathway. To determine whether AKT mediates PTK6-driven metabolic regulation, we measured the activity of LDH and FASN, two key markers of lipid synthesis and glycolysis, respectively. In PTK6-knockdown cells, treatment with SC79 further elevated LDH activity and FASN activity, whereas Colivelin treatment showed little effect (Fig. S6B). Collectively, these findings demonstrate that PTK6 regulates glucose and lipid metabolism in pancreatic cancer cells through the AKT signaling pathway, with no observable contribution from STAT3.

3.5. PTK6 modulates susceptibility to ferroptosis in pancreatic tumors by regulating fatty acid accumulation

Based on the lipidomic data, we focused on long-chain polyunsaturated fatty acids and quantified differences in lipid molecular content according to carbon chain length and degree of saturation within each lipid subclass (Fig. 5D-E). Knockdown of PTK6 induces the generation of polyunsaturated fatty acid-containing species of ceramide, phosphatidylethanolamine, triglyceride, phosphatidylserine, and sphingomyelin. Notably, palmitic acid, a direct product of fatty acid synthase, serves as one of the substrates for the synthesis of these polyunsaturated fatty acid-bearing lipid species.

siPTK6-Panc02 cells were treated in vitro with 15 μg/mL C75, a specific inhibitor of FASN, for 24 h. We found that PTK6 knockdown alone led to decreased levels of GSH, a reduced GSH/GSSG ratio, lower triglyceride (TG) content, and a decreased NADPH/$NADP^+$ ratio. Conversely, in siPTK6-Panc02 cells treated with C75 to inhibit FASN activity, increases in GSH, the GSH/GSSG ratio, and the NADPH/$NADP^+$

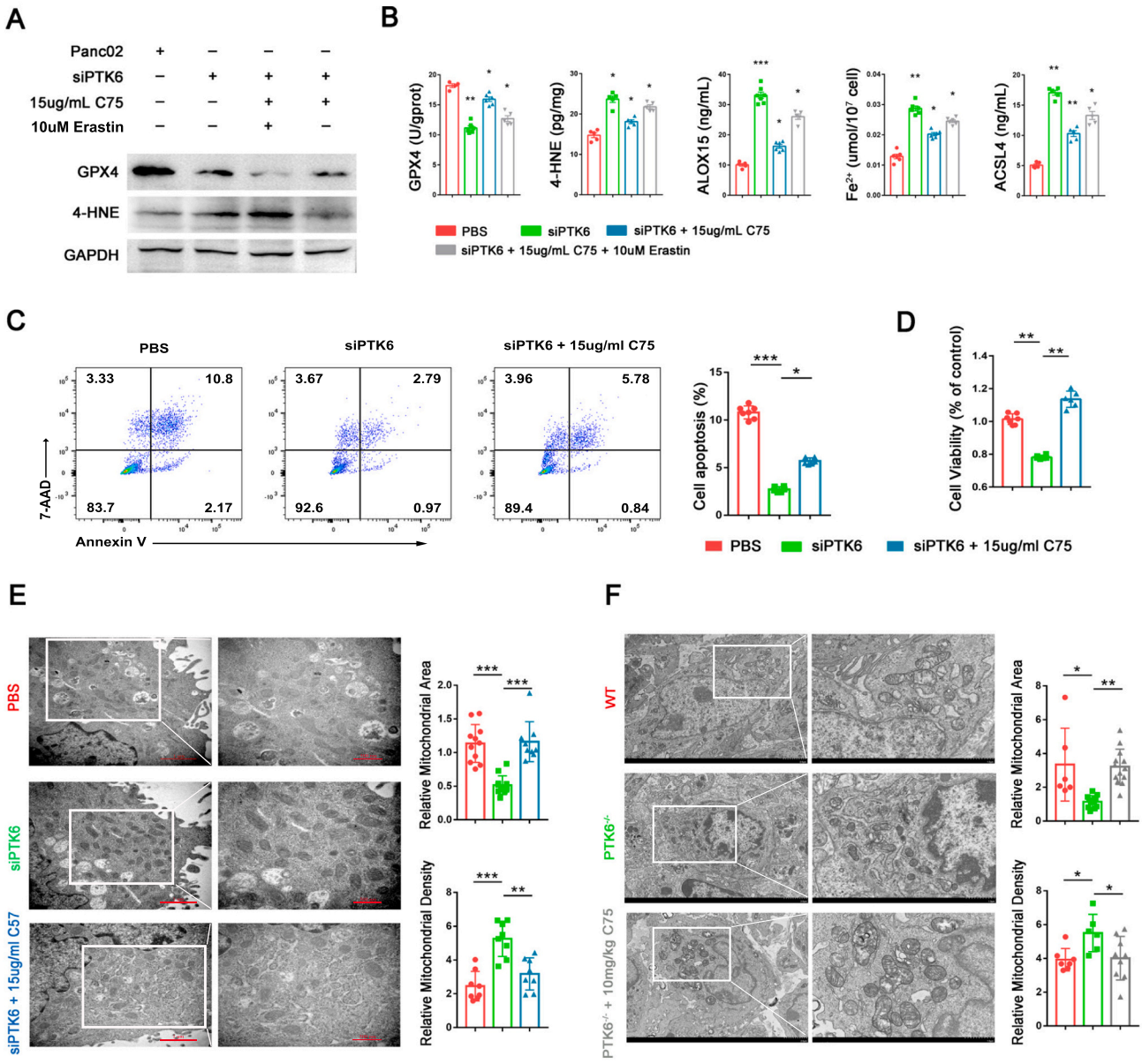

Fig. 6. PTK6 potentiates resistance to ferroptosis in pancreatic cancer cells. (A) Western blot analysis of key ferroptosis factor expression. (B) Quantitative analysis of ferroptosis marker expression by ELISA. (C) Panc02 cells with PTK6 expression knockdown were stimulated in the presence or absence of 15 μg/mL C75 for 24 h. Apoptosis rates of the cells in each group as determined by Annexin-V/PI double-staining Flow Cytometry. (D) CCK-8 assays detected the cell proliferation viability. (E and F) Cell morphology (E) and pancreatic tumor tissues (F) was observed via transmission electron microscopy. The area and density of mitochondrial is quantitative analysis by using the Image J software. $^*p < 0.05$; $^{**}p < 0.01$; $^{***}p < 0.001$ by one-way ANOVA test and were presented as mean ± SEM. n = 5–8 mice per group.

ratio was observed (Fig. 5F). This led us to hypothesize that C75 suppresses the production of palmitate, a direct product of FASN, by inhibiting FASN activity, thereby altering the output of polyunsaturated fatty acids and reversing the effects of PTK6 knockdown. To determine whether PTK6 regulates ferroptosis through lipid metabolism, we examined the expression of key ferroptosis-related proteins and markers in Panc02 cells after PTK6 knockdown. PTK6 knockdown decreased Glutathione Peroxidase 4 (GPX4) expression and increased Achaete-Scute Family bHLH Transcription Factor 4 (ACSL4) and Arachidonate 15-Lipoxygenase (ALOX15) levels compared with control cells. Consistently, PTK6 silencing led to marked elevations in Fe^{2+} accumulation and 4-Hydroxynonenal (4-HNE) levels, both indicators of lipid peroxidation (Fig. 6A-B). Treatment with C75 partially reversed these effects, whereas co-administration of the ferroptosis inducer Erastin suppress GPX4 expression and reversed ACSL4, ALOX15, Fe^{2+}, and 4-HNE levels. While these results suggest that PTK6 loss triggers ferroptosis via an effect on FASN activity, C75 confers protection by modulating the same pathway.

Consistent results were obtained from pancreatic tumors in tumor-bearing mice (Fig. S5C—D). Additionally, 24-h treatment with 15 μg/mL C75 alleviated the decrease in cell viability and the increase in apoptosis rate caused by PTK6 knockdown (Fig. 6C-D). Transmission electron microscopy revealed that siPTK6-Panc02 cells exhibited classic features of ferroptosis, including increased mitochondrial membrane density, reduced mitochondrial volume, and shrinkage of cristae. In contrast, these alterations were not observed in siPTK6-Panc02 cells treated with C75 for 24 h. (Fig. 6E). Consistent findings were observed in pancreatic tumor tissues from tumor-bearing mice. In these animals, intraperitoneal injection of C75 (10 mg/kg every other day) attenuated PTK6 knockdown-induced mitochondrial ferroptosis. (Fig. 6F). To determine whether the aforementioned regulatory effects are attributable to tumor cell-intrinsic PTK6 activity, we performed factorial design experiments and metabolic rescue experiments using palmitic acid, a direct product of FASN. $CD8^+$ T cells isolated from the pancreas of tumor-bearing mice showed that tumor-derived PTK6 increased the expression of the exhaustion markers PD-1 and Tim-3 (Fig. S6C). Total triglyceride levels were elevated in tumor tissues, with no significant contribution from host-derived PTK6 (Fig. S6D). In vitro knockdown of PTK6 significantly suppressed Panc02 cell proliferation, reduced LDH levels, and increased levels of the oxidative stress marker malondialdehyde (MDA) and Fe^{2+}, whereas palmitic acid treatment partially reversed these phenotypes (Fig. S6E). Together, these findings indicate that tumor cell-derived PTK6 exerts a positive role in promoting ferroptosis resistance through lipid metabolic regulation and may influence immune responses. TCGA analysis of PDAC patient samples showed that PTK6 mRNA expression positively correlated with ferroptosis suppressor genes (MUC1, SLC7A11, SCD, HELLS, PHGDH, and DHODH) and negatively correlated with ferroptosis promoter genes (DPP4, CS, NCOA4, PEBP1, ASCL4, GLS2, and VDAC3) (Fig. S6F-G). Validation using a mouse orthotopic pancreatic tumor model showed that, compared to wild-type mice, pancreatic tumor tissues from $PTK6^{-/-}$ mice exhibited decreased expression of MUC1, SLC7A11, SCD, HELLS, and DHODH, and increased expression of DPP4, NCOA4, and PEBP1 (Fig. S6H)

3.6. *PTK6 promotes the exhaustion of tumor-infiltrating $CD8^+$ T cells by accumulating triglycerides*

Integrating the lipidomic findings, we further investigated whether PTK6 regulates the state and function of tumor-infiltrating $CD8^+$ T cells through lipid metabolism. Compared with wild-type tumor-bearing mice, PTK6 knockout reduced triglyceride levels within the pancreatic tumor microenvironment (TME) and alleviated glycerol trioleate (a triglyceride model compound)-induced exhaustion, thereby enhancing the immune efficacy of $CD8^+$ T cells. This conclusion was supported by the elevated surface expression of the exhaustion markers PD-1 and Tim-3 on $CD8^+$ T cells in $PTK6^{-/-}$ pancreatic tumors following glycerol trioleate treatment. PTK6 knockout ameliorated this effect, increasing perforin and granzyme release and enhancing the targeted cytotoxicity of $CD8^+$ T cells. We also examined $CD4^+$ T cells and found that PTK6 knockout was accompanied by a reduction in their exhausted state (Fig. 7A-C). Similar results were observed in the spleen of pancreatic tumor-bearing mice, indicating that PTK6 knockout shifts the systemic immune landscape toward a more favorable state (Fig. 8A-C).

To assess whether triglyceride accumulation directly drives $CD8^+$ T cell exhaustion independent of tumor burden or other TME components, we established an in vitro assay. $CD8^+$ T cells isolated from spleens of wild-type C57BL/6 mice were treated with glycerol trioleate (25 μmol/L) and/or the CD36 inhibitor (SMS121, 25 μmol/L) for 24 h. Treatment with glycerol trioleate markedly upregulated the exhaustion markers PD-1 and Tim-3, along with the exhaustion-associated transcription factor thymocyte selection-associated high mobility group box protein (TOX). This was accompanied by a significant downregulation of perforin and granzyme, key effector molecules mediating $CD8^+$ T cell cytolytic function. Notably, these effects were reversed by co-treatment with SMS121 (Fig. S7A—B). These results indicate that CD36 serves as a lipid transporter that enables $CD8^+$ T cells to internalize fatty acids and other lipid species. In addition, exposure of purified $CD8^+$ T cells to Panc02-conditioned medium that contains endogenous triglycerides induced exhaustion and impaired cytotoxic activity, effects that were reversed following SMS121 administration. (Fig. S7C—D).

Therefore, PTK6 primarily promotes pancreatic tumor development by remodeling lipid metabolism, which both enhances tumor cell resistance to ferroptosis and induces exhaustion of tumor-infiltrating $CD8^+$ T cells. Consequently, targeting the mechanisms mediated by PTK6 in this process may provide a potential therapeutic strategy for clinical pancreatic cancer treatment.

4. Discussion

Pancreatic cancer is a highly aggressive malignancy of the gastrointestinal tract [26]. Although its incidence varies by geographic region, the global prevalence of pancreatic ductal adenocarcinoma (PDAC) is steadily increasing [27]. A deeper understanding of PDAC pathogenesis may not only facilitate earlier clinical detection but also guide the development of effective immunotherapeutic strategies, ultimately improving patient outcomes [28]. Protein tyrosine kinase 6 (PTK6) is an intracellular tyrosine kinase originally identified and characterized by its marked expression in invasive ductal breast carcinoma tissues [29]. Subsequent studies on the biological functions of PTK6 have established it as an important contributor to the progression of multiple cancer types [30]. In the present study, elevated PTK6 expression in pancreatic cancer was associated with reduced patient survival and correlated with key clinical characteristics of the disease. Specifically, PTK6 expression levels were higher in male patients than in female patients and were markedly increased in early-stage PDAC (Stage I–II), showing a positive correlation with tumor grade and invasive potential. These findings suggest that PTK6 plays a critical role in the early progression of pancreatic cancer and influences clinical outcomes, highlighting its potential as a diagnostic biomarker for early-stage disease. In line with these observations, an orthotopic mouse model revealed that high PTK6 expression in tumor tissue correlated with shorter survival and accelerated tumor growth. These effects were diminished in mice bearing PTK6-knockout tumors, supporting PTK6 as a promising target for early diagnosis and prognostic evaluation in pancreatic cancer progression.

Cancer-associated fibroblasts (CAFs) are a key cellular component of the pancreatic tumor microenvironment and are frequently involved in multiple pro-tumorigenic processes, including tumor initiation, metastasis, angiogenesis, and immune suppression [31,32]. These diverse roles of CAFs have greatly hindered the progress of immunotherapy against pancreatic cancer [33]. The development of PDAC is closely linked to the suppression of various immune cell populations. In

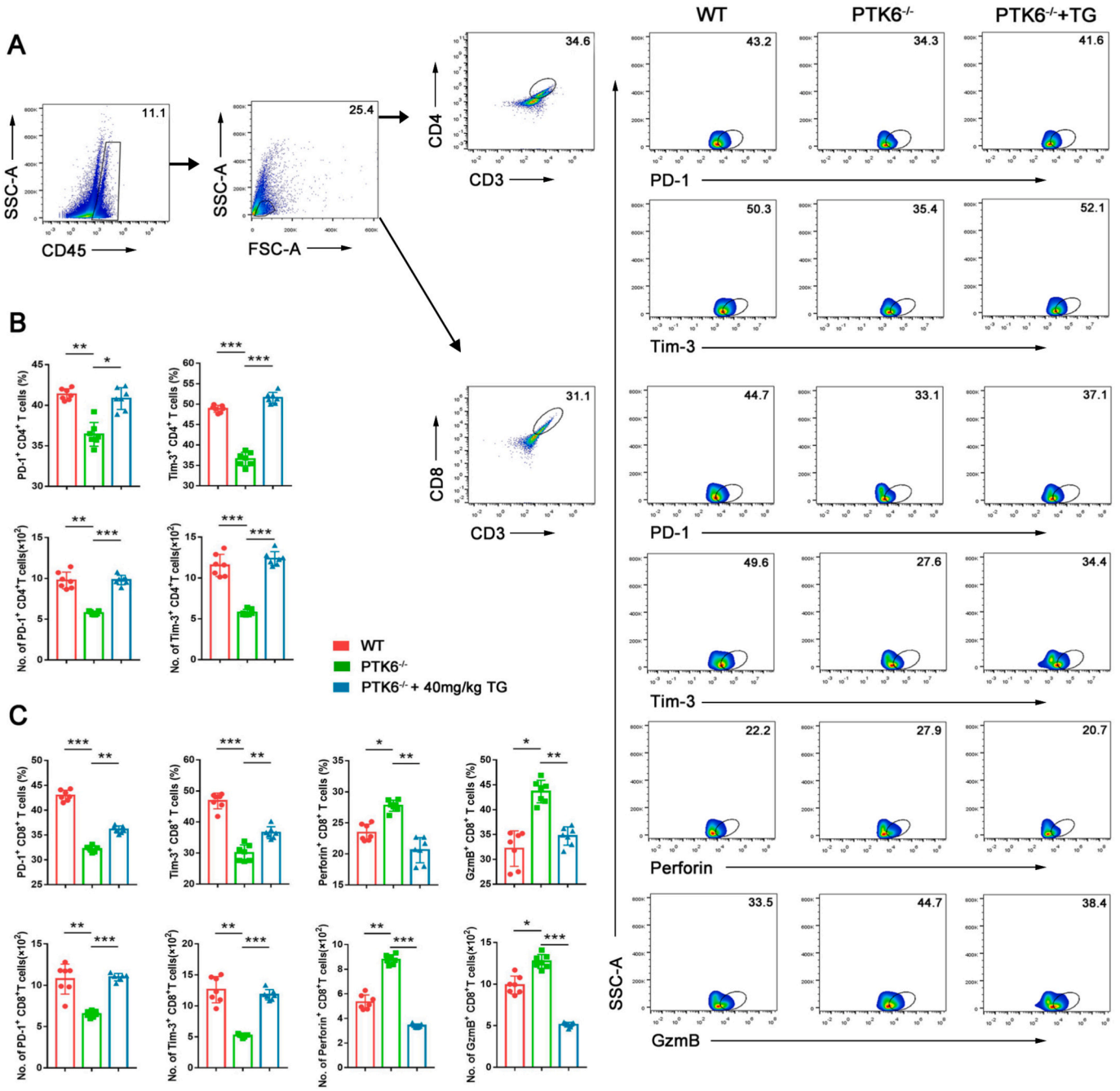

Fig. 7. PTK6 promotes triglyceride production and enhances $CD8^+$ T cell exhaustion. (A) In PTK6 knockout mice bearing orthotopic pancreatic tumors, oral gavage of glycerol trioleate (40 mg/kg, G810388, Macklin) was administered for two weeks. Pancreatic tumor tissue was then collected for flow cytometry analysis to assess $CD8^+$ T cell exhaustion. (B) Number and percentage of PD-1^+CD4^+ T cells and Tim-3^+CD4^+ T cells in pancreatic tumor tissue. (C) Number and percentage of PD-1^+CD8^+ T cells, Tim-3^+CD8^+ T cells, perforin$^+CD8^+$ T cells, and Gzm$^+CD8^+$ T cells in pancreatic tumor tissue. GzmB, granzyme B. $^*p < 0.05$; $^{**}p < 0.01$; $^{***}p < 0.001$ by one-way ANOVA test and were presented as mean ± SEM. n = 5–8 mice per group.

particular, *KRAS* mutations drive the predominant infiltration of immunosuppressive cells, whereas intertumoral T cell exhaustion, together with the activation of inhibitory immune checkpoints, collectively promotes tumor immune evasion [34,35]. We found that high PTK6 expression in the immunosuppressive tumor microenvironment of pancreatic cancer broadly affects the infiltration levels of B cells, $CD8^+$ T cells, $CD4^+$ T cells, and monocytes, accompanied by reduced expression of CD27 and CD86. CD27 serves as a costimulatory molecule that promotes the activation of effector T cells and B cells. CD86, an important molecule expressed on antigen-presenting cells, provides a critical signal for T cell proliferation and differentiation [36]. $CD8^+$ T cells are widely recognized as key effector cells in antitumor immunity. Following antigen presentation by dendritic cells (DCs), they differentiate into cytotoxic T lymphocytes (CTLs) and exert antitumor effects by secreting perforin, granzymes, and IFN-γ [37,38].

Preliminary analysis using single-cell clustering revealed that the model genes TNFSF10, PLAU, and GRAP2 exhibit robust prognostic stratification performance. In addition, age and pancreatic cancer grade were also identified as high-risk factors. PTK6, meanwhile, acts as a high-risk factor associated with poor prognosis in pancreatic cancer. The Wound Healing (C1), IFN-γ-dominant (C2), and TGF-β-dominant (C6) subtypes were mainly enriched in the high-risk group, whereas the

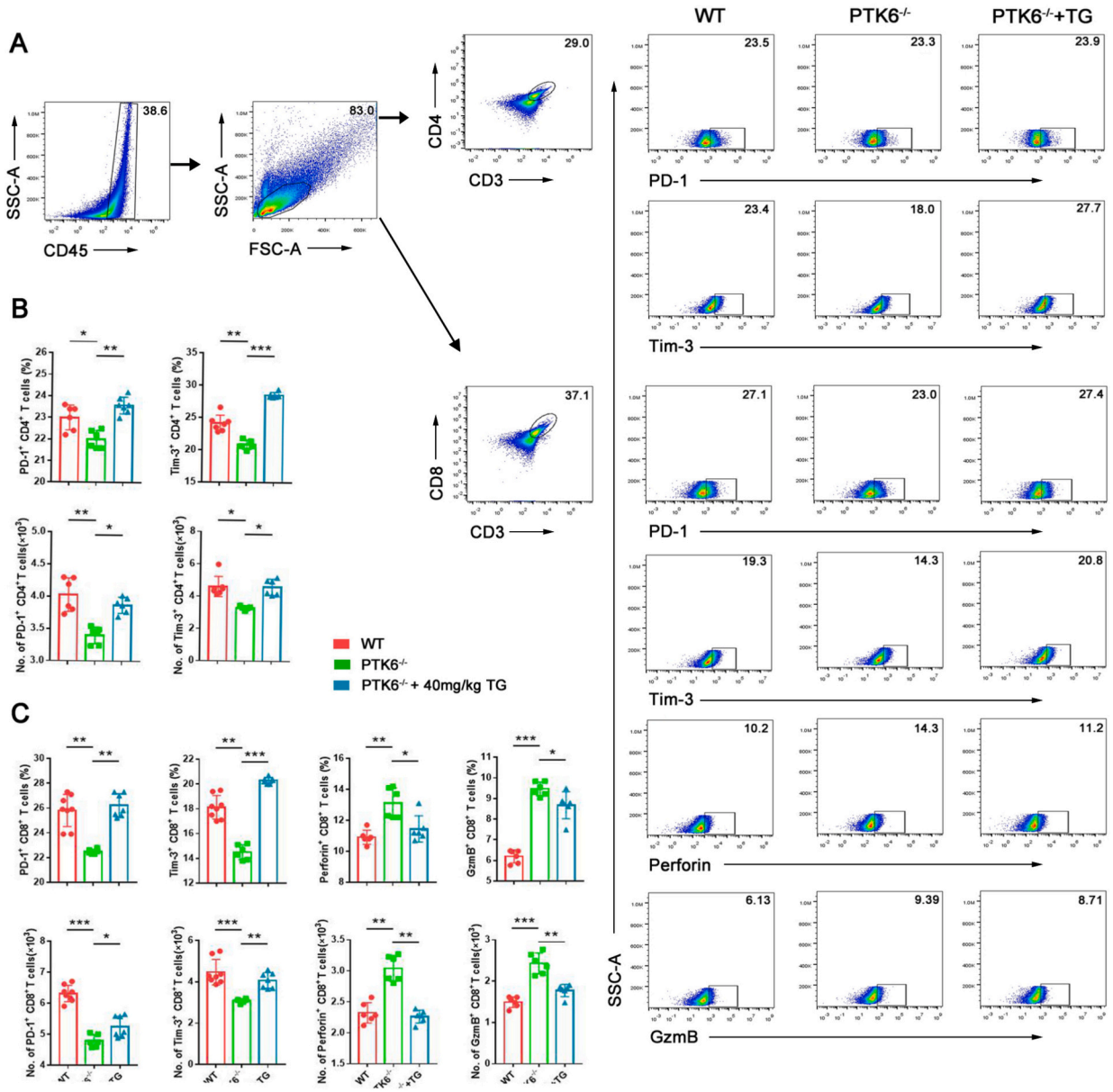

Fig. 8. PTK6 drives $CD8^+$ T cell exhaustion in the systemic immune landscape through modulation of triglyceride content. (A) In PTK6 knockout mice bearing orthotopic pancreatic tumors, oral gavage of glycerol trioleate (40 mg/kg, G810388, Macklin) was administered for two weeks. Spleen tissue was then collected for flow cytometry analysis to assess $CD8^+$ T cell exhaustion. (B) Number and percentage of PD-1^+CD4^+ T cells and Tim-3^+CD4^+ T cells in spleen tissue. (C) Number and percentage of PD-1^+CD8^+ T cells, Tim-3^+CD8^+ T cells, perforin$^+CD8^+$ T cells, and Gzm$^+CD8^+$ T cells in spleen tissue. GzmB, granzyme B. $^*p < 0.05$; $^{**}p < 0.01$; $^{***}p < 0.001$ by one-way ANOVA test and were presented as mean ± SEM. n = 5–8 mice per group.

Inflammatory (C3) subtype was enriched in the low-risk group [39–41]. These findings suggest that PTK6 promotes tumor growth and immune evasion, with 49% of cases classified as the wound healing (C1) subtype. A highly immunosuppressive tumor microenvironment (27%, C2 subtype) and compensatory immunosuppression affecting $CD8^+$ T cells (13%, C6 subtype) were also observed. Furthermore, PTK6 alters the antitumor immune landscape (11%, C3 subtype), rendering $CD8^+$ T cells incapable of mounting an effective antitumor response. These observations corroborate the well-recognized characterization of pancreatic cancer as an immunologically "cold" tumor. GSEA enrichment analysis revealed that high PTK6 expression remodels carbohydrate and lipid metabolism. Previous studies have shown that elevated fatty acid synthase (FASN) in pancreatic tumors catalyzes the NADPH-dependent conversion of acetyl-CoA and malonyl-CoA to palmitate, thereby promoting lipid accumulation. This metabolic process supports tumor growth and diminishes the antiproliferative efficacy of targeted agents [42].

These findings prompted us to further investigate how PTK6 regulates pancreatic tumor progression. Lipidomic analysis combined with experimental validation revealed that PTK6, through the activity of FASN, alters the production ratio of polyunsaturated fatty acids, thereby enhancing ferroptosis resistance in pancreatic cancer cells.

Ferroptosis is an iron-dependent form of cell death driven by peroxidation of membrane lipids [43]. Our study shows that PTK6 selectively activates AKT phosphorylation and regulates glycolytic and lipid metabolic remodeling by modulating the activities of LDH and FASN. Knockdown of PTK6 reduces the antioxidant capacity of GPX4 and increases the level of oxidized glutathione. Meanwhile, the levels of ACSL4 and ALOX15, key proteins in ferroptosis, are elevated. The increases in malondialdehyde (MDA) and 4-hydroxynonenal (4-HNE), core products of lipid peroxidation, indicate functional lipid peroxidation injury. Moreover, the accumulation of Fe^{2+} serves as a catalyst that initiates the

ferroptosis cascade and directly drives lipid peroxidation [44]. Consequently, the proliferative activity of pancreatic tumor cells declines, and the mitochondria exhibit typical ferroptosis features, including increased membrane density and reduced volume.

In metabolic rescue experiments, the direct FASN product palmitate enabled polyunsaturated fatty acid accumulation and partially reversed the phenotypic changes induced by the FASN inhibitor C75. These findings indicate that tumor cell-derived PTK6 plays a positive role in ferroptosis resistance through the regulation of lipid metabolism.

Previous studies have largely focused on the notion that the progression of pancreatic cancer heavily depends on dysregulated cholesterol metabolism. Cholesterol binds to and induces palmitoylation of Frizzled 5, thereby driving the Wnt/β-catenin signaling pathway to promote tumor growth [45]. Tumor cells promote the uptake of cholesterol by $CD8^+$ T cells, which accelerates their senescence. Concurrently, the accumulation of lactate disrupts the tricarboxylic acid (TCA) cycle in immune cells [46–48]. Triglycerides and monounsaturated fatty acids inhibit lipid peroxidation and reduce reactive oxygen species (ROS) generation, thereby promoting cancer cell survival [49]. Our findings indicate that PTK6 enhances the capacity of pancreatic tumor cells to produce triglycerides, leading to elevated triglyceride levels in the tumor microenvironment. Tumor-infiltrating $CD8^+$ T cells, after taking up lipids via CD36, exhibit an exhausted phenotype characterized by high expression of PD-1 and Tim-3, activation of TOX (a core transcription factor driving exhaustion), and reduced cytotoxic activity (as evidenced by decreased secretion of perforin and granzymes). These changes may compromise antitumor immunity in the systemic immune landscape and help tumors evade immune control. This cancer-associated immunosuppressive process drives pancreatic tumors toward a low-immunogenicity phenotype, thereby providing an opportunity for immune evasion.

In summary, our findings suggest that PTK6 may serve as both a potential prognostic biomarker and a candidate mechanistic target in pancreatic cancer, where it plays a dual role within the immunosuppressive “cold” tumor microenvironment. PTK6 drives aberrant tumor progression by reprogramming lipid metabolism, leading to reduced levels of long-chain polyunsaturated fatty acids (PUFAs) and suppression of ferroptosis driven by lipid peroxidation. Concurrently, PTK6-driven triglyceride accumulation in the tumor microenvironment directly induces T cell dysfunction, thereby fueling immunosuppression and tumor immune evasion. Although our findings identify PTK6 as a potential biomarker, future studies using orthotopic pancreatic cancer models are warranted to investigate the combination of PTK6 inhibition with immune checkpoint blockade and to evaluate potential synergistic effects. Accordingly, targeting PTK6 in conjunction with immune checkpoint inhibition and restoring T cell effector function should be prioritized in future research, aiming to overcome drug resistance in pancreatic cancer and provide a theoretical basis for improving clinical outcomes.

CRediT authorship contribution statement

Rui Zheng: Writing – original draft, Visualization, Validation, Methodology, Investigation, Funding acquisition, Formal analysis, Data curation. **Si Wang:** Project administration, Funding acquisition. **Dan Li:** Validation, Software, Methodology, Investigation. **Xing Tian:** Resources, Methodology. **Lifeng Sun:** Validation, Software, Methodology. **Jiao Wang:** Resources, Investigation. **Yuchang Wang:** Supervision, Resources. **Xuyi Pan:** Resources, Investigation. **Yifan Liang:** Resources, Investigation. **Zhihang Yang:** Writing – review & editing, Supervision, Project administration, Methodology, Investigation, Funding acquisition, Conceptualization.

Ethics approval and consent to participate

This research was approved by the Ethics Committee of China Medical University of Science and Technology.

Funding

This work was supported by the joint program of the Natural Science Foundation of Liaoning Province (2024-BSLH-292), the Shenyang Medical College Undergraduate Research Program (20249080) and the College Students' Innovation and Entrepreneurship Training Program (20259137).

Declaration of competing interest

The authors declare that they have no known competing financial interests or personal relationships that could have appeared to influence the work reported in this paper.

Acknowledgments

We are grateful to the Laboratory of Pathogenic Biology at China Medical University for their technical assistance throughout this study.

Appendix A. Supplementary data

Supplementary data to this article can be found online at https://doi.org/10.1016/j.intimp.2026.116744.

Data availability

The lipidomics data have been deposited to the MetaboLights repository with the identifier MTBLS13981.

References

[1] A.P. Klein, Pancreatic cancer epidemiology: understanding the role of lifestyle and inherited risk factors, Nat. Rev. Gastroenterol. Hepatol. 18 (2021) 493–502, https://doi.org/10.1038/s41575-021-00457-x.
[2] Thomas F, S., Ammar A, J., Atsushi, O., Bas Groot, K., Thomas, S., Johanna W, W., and Marc G, B., Pancreatic cancer, Lancet 405 (2025),doi:https://doi.org/10.1016/s0140-6736(25)00261-2.
[3] Jie, C., Hongda, C., Ming, L., Yuhan, Z., Bin, L., Lei, Y., Taiping, Z., Min, D., and Yupei, Z., Advances in the epidemiology of pancreatic cancer: trends, risk factors, screening, and prognosis, Cancer Lett. 520 (2021),doi:https://doi.org/10.1016/j.canlet.2021.06.027.
[4] L. Zhang, S. Sanagapalli, A. Stoita, Challenges in diagnosis of pancreatic cancer, World J. Gastroenterol. 24 (2018) 2047–2060, https://doi.org/10.3748/wjg.v24.i19.2047.
[5] C. Qin, G. Yang, J. Yang, B. Ren, H. Wang, G. Chen, F. Zhao, L. You, W. Wang, Y. Zhao, Metabolism of pancreatic cancer: paving the way to better anticancer strategies, Mol. Cancer 19 (2020) 50, https://doi.org/10.1186/s12943-020-01169-7.
[6] C.J. Halbrook, C.A. Lyssiotis, M. Pasca di Magliano, A. Maitra, Pancreatic cancer: advances and challenges, Cell 186 (2023) 1729–1754, https://doi.org/10.1016/j.cell.2023.02.014.
[7] M.H. Sherman, G.L. Beatty, Tumor microenvironment in pancreatic cancer pathogenesis and therapeutic resistance, Annu. Rev. Pathol. 18 (2023) 123–148, https://doi.org/10.1146/annurev-pathmechdis-031621-024600.
[8] Y. Fu, J. Tao, T. Liu, Y. Liu, J. Qiu, D. Su, R. Wang, W. Luo, Z. Cao, G. Weng, et al., Unbiasedly decoding the tumor microenvironment with single-cell multiomics analysis in pancreatic cancer, Mol. Cancer 23 (2024) 140, https://doi.org/10.1186/s12943-024-02050-7.
[9] A.H. Morrison, K.T. Byrne, R.H. Vonderheide, Immunotherapy and prevention of pancreatic cancer, Trends Cancer 4 (2018) 418–428, https://doi.org/10.1016/j.trecan.2018.04.001.
[10] Dimitrios, S., Nikolaos, C., Christo, K., Panagiota, E., Evangelos, K., Efthymios, G., Dimitrios, Z., Amanda, P., and Michalis V, K., Immunotherapy for pancreatic cancer: a 2020 update, Cancer Treat. Rev. 86 (2020),doi:https://doi.org/10.1016/j.ctrv.2020.102016.
[11] B. Liu, X. Yao, C. Zhang, Y. Liu, L. Wei, Q. Huang, M. Wang, Y. Zhang, D. Hu, W. Wu, PTK6 inhibits autophagy to promote uveal melanoma tumorigenesis by binding to SOCS3 and regulating mTOR phosphorylation, Cell Death Dis. 14 (2023) 55, https://doi.org/10.1038/s41419-023-05590-w.
[12] Y.P. Hsieh, K.C. Chen, M.Y. Chen, L.Y. Huang, A.Y. Su, W.F. Chiang, W.T. Huang, T.T. Huang, Epigenetic deregulation of protein tyrosine kinase 6 promotes carcinogenesis of oral squamous cell carcinoma, Int. J. Mol. Sci. 23 (2022), https://doi.org/10.3390/ijms23094495.

[13] Bingyuan, C., Bowen, L., Junnan, C., Wenjing, L., Ning, M., Jianquan, L., Ruizhi, F., Qihang, H., Hu, S., Yixin, X., et al., PTK6 drives HNRNPH1 phase separation to activate autophagy and suppress apoptosis in colorectal cancer, Autophagy 21 (2025),doi:https://doi.org/10.1080/15548627.2025.2481001.
[14] M.B. Gilic, A.L. Tyner, Targeting protein tyrosine kinase 6 in cancer, Biochim. Biophys. Acta Rev. Cancer 1874 (2020) 188432, https://doi.org/10.1016/j.bbcan.2020.188432.
[15] Y. Zheng, Z. Wang, W. Bie, P.M. Brauer, B.E. Perez White, J. Li, V. Nogueira, P. Raychaudhuri, N. Hay, D.A. Tonetti, et al., PTK6 activation at the membrane regulates epithelial-mesenchymal transition in prostate cancer, Cancer Res. 73 (2013) 5426–5437, https://doi.org/10.1158/0008-5472.CAN-13-0443.
[16] T.M. Regan Anderson, S.H. Ma, G.V. Raj, J.A. Cidlowski, T.M. Helle, T.P. Knutson, R.I. Krutilina, T.N. Seagroves, C.A. Lange, Breast tumor kinase (Brk/PTK6) is induced by HIF, glucocorticoid receptor, and PELP1-mediated stress signaling in triple-negative breast cancer, Cancer Res. 76 (2016) 1653–1663, https://doi.org/10.1158/0008-5472.CAN-15-2510.
[17] P.S. Mathur, J.J. Gierut, G. Guzman, H. Xie, R.M. Xicola, X. Llor, M.I. Chastkofsky, A.O. Perekatt, A.L. Tyner, Kinase-dependent and -independent roles for PTK6 in colon cancer, Mol. Cancer Res. 14 (2016) 563–573, https://doi.org/10.1158/1541-7786.MCR-15-0450.
[18] Y.D. Lang, H.Y. Chen, C.M. Ho, J.H. Shih, E.C. Hsu, R. Shen, Y.C. Lee, J.W. Chen, C. Y. Wu, H.W. Yeh, et al., PSPC1-interchanged interactions with PTK6 and beta-catenin synergize oncogenic subcellular translocations and tumor progression, Nat. Commun. 10 (2019) 5716, https://doi.org/10.1038/s41467-019-13665-6.
[19] H. Ono, M.D. Basson, H. Ito, PTK6 promotes cancer migration and invasion in pancreatic cancer cells dependent on ERK signaling, PloS One 9 (2014) e96060, https://doi.org/10.1371/journal.pone.0096060.
[20] Hiroaki, O., Marc D, B., and Hiromichi, I., PTK6 potentiates gemcitabine-induced apoptosis by prolonging s-phase and enhancing DNA damage in pancreatic cancer, Mol. Cancer Res. 13 (2015),doi:https://doi.org/10.1158/1541-7786.Mcr-15-0034.
[21] J. Vivian, A.A. Rao, F.A. Nothaft, C. Ketchum, J. Armstrong, A. Novak, J. Pfeil, J. Narkizian, A.D. Deran, A. Musselman-Brown, et al., Toil enables reproducible, open source, big biomedical data analyses, Nat. Biotechnol. 35 (2017) 314–316, https://doi.org/10.1038/nbt.3772.
[22] R. Zheng, S. Wang, J. Wang, M. Zhou, Q. Shi, B. Liu, Neuromedin u regulates the anti-tumor activity of CD8(+) t cells and glycolysis of tumor cells in the tumor microenvironment of pancreatic ductal adenocarcinoma in an NMUR1-dependent manner, Cancer Sci. 115 (2024) 334–346, https://doi.org/10.1111/cas.16024.
[23] X. Bian, Y.T. Xiao, T. Wu, M. Yao, L. Du, S. Ren, J. Wang, Microvesicles and chemokines in tumor microenvironment: mediators of intercellular communications in tumor progression, Mol. Cancer 18 (2019) 50, https://doi.org/10.1186/s12943-019-0973-7.
[24] L.A. Rojas, Z. Sethna, K.C. Soares, C. Olcese, N. Pang, E. Patterson, J. Lihm, N. Ceglia, P. Guasp, A. Chu, et al., Personalized RNA neoantigen vaccines stimulate t cells in pancreatic cancer, Nature 618 (2023) 144–150, https://doi.org/10.1038/s41586-023-06063-y.
[25] B. Wu, S. Xi, Bioinformatics analysis of differentially expressed genes and pathways in the development of cervical cancer, BMC Cancer 21 (2021) 733, https://doi.org/10.1186/s12885-021-08412-4.
[26] Y. Wang, G. Yang, L. You, J. Yang, M. Feng, J. Qiu, F. Zhao, Y. Liu, Z. Cao, L. Zheng, et al., Role of the microbiome in occurrence, development and treatment of pancreatic cancer, Mol. Cancer 18 (2019) 173, https://doi.org/10.1186/s12943-019-1103-2.
[27] L.D. Wood, M.I. Canto, E.M. Jaffee, D.M. Simeone, Pancreatic cancer: pathogenesis, screening, diagnosis, and treatment, Gastroenterology 163 (2022) 386–402 e381, https://doi.org/10.1053/j.gastro.2022.03.056.
[28] E.M. Stoffel, R.E. Brand, M. Goggins, Pancreatic cancer: changing epidemiology and new approaches to risk assessment, early detection, and prevention, Gastroenterology 164 (2023) 752–765, https://doi.org/10.1053/j.gastro.2023.02.012.
[29] C. Liu, Z. Pan, Q. Chen, Z. Chen, W. Liu, L. Wu, M. Jiang, W. Lin, Y. Zhang, W. Lin, et al., Pharmacological targeting PTK6 inhibits the JAK2/STAT3 sustained stemness and reverses chemoresistance of colorectal cancer, J. Exp. Clin. Cancer Res. 40 (2021) 297, https://doi.org/10.1186/s13046-021-02059-6.
[30] A.R. Dwyer, C.P. Kerkvliet, R.I. Krutilina, H.C. Playa, D.N. Parke, W.A. Thomas, B. A. Smeester, B.S. Moriarity, T.N. Seagroves, C.A. Lange, Breast tumor kinase (Brk/PTK6) mediates advanced cancer phenotypes via SH2-domain dependent activation of RhoA and aryl hydrocarbon receptor (AhR) signaling, Mol. Cancer Res. 19 (2021) 329–345, https://doi.org/10.1158/1541-7786.MCR-20-0295.
[31] Bruno, B., Joseph E, G., and Manuel, H., Facts and hopes in immunotherapy of pancreatic cancer, Clin. Cancer Res. 28 (2022),doi:https://doi.org/10.1158/1078-0432.Ccr-21-3452.
[32] X. Mao, J. Xu, W. Wang, C. Liang, J. Hua, J. Liu, B. Zhang, Q. Meng, X. Yu, S. Shi, Crosstalk between cancer-associated fibroblasts and immune cells in the tumor microenvironment: new findings and future perspectives, Mol. Cancer 20 (2021) 131, https://doi.org/10.1186/s12943-021-01428-1.
[33] Giulia, B., and David A, T., Diversity and biology of cancer-associated fibroblasts, Physiol. Rev. 101 (2020),doi:https://doi.org/10.1152/physrev.00048.2019.
[34] W.J. Ho, E.M. Jaffee, L. Zheng, The tumour microenvironment in pancreatic cancer - clinical challenges and opportunities, Nat. Rev. Clin. Oncol. 17 (2020) 527–540, https://doi.org/10.1038/s41571-020-0363-5.
[35] Elisabeth, H., Soeren M, B., Ihsan Ekin, D., Shiv K, S., Thomas M, G., Volker, E., and Albrecht, N., Microenvironmental determinants of pancreatic cancer, Physiol. Rev. 100 (2020),doi:https://doi.org/10.1152/physrev.00042.2019.
[36] G. Huidong, W. Bixia, W. Zhigui, Z. Qi, J. Xinya, Z. Fangqing, Z. Jingrui, F. Shuang, Z. Yang, X. Zheng-Li, et al., CD8(+)HLA-DR(+)CD27(+) t cells define a population of naturally occurring regulatory precursors in humans, Sci. Adv. 11 (2025), https://doi.org/10.1126/sciadv.adw1702.
[37] S. Zhang, M. Rozell, R.K. Verma, D.I. Albu, D. Califano, J. VanValkenburgh, A. Merchant, J. Rangel-Moreno, T.D. Randall, N.A. Jenkins, et al., Antigen-specific clonal expansion and cytolytic effector function of CD8+ t lymphocytes depend on the transcription factor bcl11b, J. Exp. Med. 207 (2010) 1687–1699, https://doi.org/10.1084/jem.20092136.
[38] B. Minghui, Z. Youwei, L. Haichao, S. Baowei, Z. Yong, H. Hua, CXCR5(+) CD8(+) t cells potently infiltrate pancreatic tumors and present high functionality, Exp. Cell Res. 361 (2017), https://doi.org/10.1016/j.yexcr.2017.09.039.
[39] J. Liu, Q. Liu, X. Zhang, M. Cui, T. Li, Y. Zhang, Q. Liao, Immune subtyping for pancreatic cancer with implication in clinical outcomes and improving immunotherapy, Cancer Cell Int. 21 (2021) 137, https://doi.org/10.1186/s12935-021-01824-z.
[40] A. Zhang, K. Miao, H. Sun, C.X. Deng, Tumor heterogeneity reshapes the tumor microenvironment to influence drug resistance, Int. J. Biol. Sci. 18 (2022) 3019–3033, https://doi.org/10.7150/ijbs.72534.
[41] Z. Siyi, Z. Lei, J. Cen, L. Fanlu, Y. Ying, D. Xiaxing, Z. Jiao, C. Hao, J. Lingxi, C. Xueyan, et al., Driver mutation subtypes involve with differentiated immunophenotypes influencing pancreatic cancer outcomes, Cancer Lett. 599 (2024), https://doi.org/10.1016/j.canlet.2024.217134.
[42] S. Tadros, S.K. Shukla, R.J. King, V. Gunda, E. Vernucci, J. Abrego, N.V. Chaika, F. Yu, A.J. Lazenby, L. Berim, et al., De novo lipid synthesis facilitates gemcitabine resistance through endoplasmic reticulum stress in pancreatic cancer, Cancer Res. 77 (2017) 5503–5517, https://doi.org/10.1158/0008-5472.CAN-16-3062.
[43] S.J. Dixon, J.A. Olzmann, The cell biology of ferroptosis, Nat. Rev. Mol. Cell Biol. 25 (2024) 424–442, https://doi.org/10.1038/s41580-024-00703-5.
[44] N. Abdukarimov, K. Kokabi, J. Kunz, Ferroptosis and iron homeostasis: molecular mechanisms and neurodegenerative disease implications, Antioxidants (Basel) 14 (2025), https://doi.org/10.3390/antiox14050527.
[45] S. Zheng, J. Lin, Z. Pang, H. Zhang, Y. Wang, L. Ma, H. Zhang, X. Zhang, M. Chen, X. Zhang, et al., Aberrant cholesterol metabolism and Wnt/beta-catenin signaling coalesce via Frizzled5 in supporting cancer growth, Adv Sci (Weinh). 9 (2022) e2200750, https://doi.org/10.1002/advs.202200750.
[46] W. Runxian, L. Zhenya, F. Zhiyao, Z. Hanxiang, Lipid metabolism reprogramming of CD8(+) t cell and therapeutic implications in cancer, Cancer Lett. 567 (2023), https://doi.org/10.1016/j.canlet.2023.216267.
[47] Ma, X., Bi, E., Lu, Y., Su, P., Huang, C., Liu, L., Wang, Q., Yang, M., Kalady, M.F., Qian, J., et al., Cholesterol induces CD8(+) t cell exhaustion in the tumor microenvironment, Cell Metab. 30 (2019) 143-156 e145,doi:https://doi.org/10.1016/j.cmet.2019.04.002.
[48] X. Ma, L. Xiao, L. Liu, L. Ye, P. Su, E. Bi, Q. Wang, M. Yang, J. Qian, Q. Yi, CD36-mediated ferroptosis dampens intratumoral CD8(+) t cell effector function and impairs their antitumor ability, Cell Metab. 33 (2021), https://doi.org/10.1016/j.cmet.2021.02.015, 1001-1012 e1005.
[49] M.A. Freitas-Cortez, F. Masrorpour, H. Jiang, I. Mahmud, Y. Lu, A. Huang, L. K. Duong, Q. Wang, T.A. Voss, C.S. Kettlun Leyton, et al., Cancer cells avoid ferroptosis induced by immune cells via fatty acid binding proteins, Mol. Cancer 24 (2025) 40, https://doi.org/10.1186/s12943-024-02198-2.